

# Prediction of the Creep of Heterogeneous Polymer Blends: Rubber-Toughened Polypropylene/Poly(Styrene-*co*-Acrylonitrile)

JAN KOLAŘÍK\*

*Institute of Macromolecular Chemistry  
Academy of Sciences of the Czech Republic  
162 06 Prague 6, Czech Republic*

LUCA FAMBRI, ALESSANDRO PEGORETTI, and AMABILE PENATI

*Department of Materials Engineering  
University of Trento  
38050 Trento, Italy*

PAOLO GOBERTI

*Basell Polyolefins  
44100 Ferrara, Italy*

A previously proposed predictive format for elastic, storage and loss moduli is extended for the time-dependent compliance  $D_b(t)$  of polymer blends. The format employs a two-parameter equivalent box model (EBM) and the data on the phase continuity of components in blends obtained by using modified general equations of the percolation theory. As input data, the compliances  $D_1(t)$  and  $D_2(t)$  and the critical volume fractions  $v_{1cr}$  and  $v_{2cr}$  (delimiting the interval of phase co-continuity in blends) of components are sufficient. To describe the effect of time on  $D_1(t)$ ,  $D_2(t)$  and  $D_b(t)$  within the linear stress-strain region, a routinely used empirical equation was found suitable. Applicability of the proposed format is demonstrated on rubber-toughened polypropylene/poly(styrene-*co*-acrylonitrile) blends consisting of components with markedly different viscoelastic properties. The proposed predictive format fits fairly well the creep behavior of blends over the interval 0.1–10,000 minutes.

## INTRODUCTION

Although preparation of polymer blends ranks among the cost-effective ways of the upgrading of common polymers, the prediction of resultant physical properties of blends is still under development. As generally recognized, possible applications of polymeric materials are frequently determined by their mechanical properties; thus, it is highly desirable to anticipate selected properties of intended blends as functions of composition. In our previous papers (1–14) we have proposed and verified a versatile predictive scheme for modulus  $E_b$ , yield strength  $S_{yb}$ , tensile

strength  $S_{ub}$  and permeability  $P_b$  of two- or three-component heterogeneous polymer blends. Recently, the format was extended for storage  $E'$  and loss  $E''$  moduli of binary blends (15). An essential feature of the proposed predictive scheme is that all considered properties of a blend are interrelated because they are calculated for a certain phase structure by means of an identical set of input parameters.

Whenever products made of thermoplastics are exposed to a long-lasting dead load (constant external force), their propensity to creep—which considerably affects their dimensional stability—becomes a most important characteristic. Thus, the acquisition of creep data over appropriate periods of time and their analysis are undoubtedly of great practical interest (16).

\*Corresponding author: E-mail: kolarik@imc.cas.cz

Although the creep of many polymers has been described, much less is known about the creep of polymer blends. Even recent monographs on polymer blends (17–20) pay no attention to this important topic. So far, creep behavior has been mainly studied of blends containing dispersed minority components or rubbery particles (impact modifiers) (21–27). However, such two-component materials were treated in the same way as individual polymers (simple materials) and no models were attempted to describe the creep of blends as a sum of the contributions of constituents. Obviously, models for particulate composites (16) can be modified for polymer blends with a fully dispersed minority component; on the other hand, a dispersed polymer component showing creep, yielding and plastic deformation is very different from an ordinary inorganic filler (or reinforcement) mainly used in composites and characterized by “zero” permeability, compliance and plastic deformation.

Recent studies (3–7, 11–15, 28–30) have clearly shown that a minority component in two-component heterogeneous blends usually assumes partial continuity at a critical volume fraction as low as  $0.1 < v_{1cr}$  (or  $v_{2cr}$ )  $< 0.2$ . In a wide central interval, say  $0.15 < v_1$  (or  $v_2$ )  $< 0.85$ , phase structures with partially co-continuous constituents are typical of polymer blends. However, various models for composites with continuous fibers (31, 32) are not applicable to polymer blends because the latter materials are isotropic. Thus, development of a predictive format for selected mechanical properties of polymer blends and its experimental verification remain basic problems of materials engineering since it is evident that a reliable prediction of properties of envisaged blends can bring savings of time and financial means. Such a predictive format should allow for (i) the respective property of components, (ii) real phase structures encompassing a wide interval of the co-continuity of phases and, whenever necessary, (iii) the strength of interfacial adhesion. The objective of this paper is to extend the previously proposed predictive format for the time-dependent compliance of heterogeneous binary blends because, at present, there is no good way of predicting the creep of a blend with the aid of the creep data of constituents. The predictive format and the effect of critical volume fractions (percolation thresholds (33)) are verified on model blends consisting of impact-resistant polypropylene and poly(styrene-co-acrylonitrile) where the components have markedly different elastic and viscoelastic properties (15).

## EXPERIMENTAL

### Materials

A rubber-toughened polypropylene (RTPP), Moplen EPT30R (Montell, Ferrara, Italy), is a heterophase copolymer consisting of 88% of polypropylene and 12% of ethylene/propylene (65/35) rubber (density 0.92 g/cm<sup>3</sup>). Poly(styrene-co-acrylonitrile) (SAN) Kostil B255 (Enichem, Mantova, Italy) is a copolymer containing

about 24% of acrylonitrile (density 1.07 g/cm<sup>3</sup>). Polymers were mixed in a Banbury mixer (chamber 4.3 l; 164 rpm) at 175°C for 3.5 min. The produced pellets were used for feeding a Negri-Bossi injection molding machine (barrel temperature: 235°C; injection pressure: 200 bar) to produce test specimens for the measurements of mechanical properties. Test specimens were stored at room temperature for about ten months before the creep tests were initiated to eliminate any effect of physical aging in the course of creeping. Glass transition temperatures of EPR, PP and SAN determined by DMTA (15) are about  $T_g = -50, 0$  and 100°C, respectively. Microphotographs visualizing the phase structure of studied blends were discussed in our previous paper (15).

### Creep Measurements

Tensile measurements were performed with the aid of a simple apparatus equipped with a mechanical stress amplifier (lever) 10:1. The length of specimens was measured with mechanical strain gauge with an accuracy of 2 μm, i.e., of about 0.002% (initial distance between grips: 90 mm; cross section: 10 mm × 4 mm). Mechanical conditioning before each creep measurement consisted in applying a stress (for 1 min), which produced a strain larger than the expected final strain attained in the following short-term or long-term measurement; the recovery period after the conditioning was more than 1 h. Short-term tensile creep measurements in the interval 0.1–100 min were performed at gradually increasing stress levels (between 2.7 and 27 MPa) in order to ascertain the linearity limit between stress and strain. Each short-term creep measurement was followed by a 22 h recovery before another creep test (at an increased stress) was initiated. Long-term tensile creep experiments under a selected stress extended from 0.1 to 10,000 min. Three-point flexural creep was measured over the period 0.1–10 000 min by using test specimens 110 mm × 10 mm × 4 mm (the distance between supports was 80 mm). All creep tests were implemented at room temperature, i.e., 21–23°C. At the time of testing, the specimens were about one year old so that no interfering effect of physical aging was considered.

## DESCRIPTIVE FORMAT FOR CREEP OF BLENDS

### Empirical Functions for the Creep of Polymers

Creep deformation  $\varepsilon$  of polymers depends on time  $t$ , acting stress  $\sigma$  and temperature  $T$  (sometimes also on other effects, such as physical aging and relative humidity). In general,  $\varepsilon(t, \sigma, T)$  consists of three components (7): (i) *elastic* (instantaneous) deformation  $\varepsilon_o(\sigma, T)$ ; (ii) *viscoelastic* (reversible) deformation  $\varepsilon_v(t, \sigma, T)$ ; (iii) *plastic* (irreversible) deformation  $\varepsilon_p(t, \sigma, T)$ :

$$\varepsilon(t, \sigma, T) = \varepsilon_o(\sigma, T) + \varepsilon_v(t, \sigma, T) + \varepsilon_p(t, \sigma, T). \quad (1a)$$

However, in practice the conditions should be avoided where  $\varepsilon_p(t, \sigma, T) > 0$  because any plastic deformation

can be viewed as an irreversible damage of a product. In terms of the tensile compliance  $D = \epsilon/\sigma$  we obtain

$$D(t, \sigma, T) = D_o(\sigma, T) + D_v(t, \sigma, T) + D_p(t, \sigma, T). \quad (1b)$$

If an experimental creep curve can be fitted by a suitable equation, then storage of experimental data, evaluation of creep rate, interpolation or extrapolation of creep deformation, etc., are facilitated. Several attempts have been made (16, 34–36) to express creep deformation as a product of the functions of time, stress and temperature, i.e.,  $\epsilon(t, \sigma, T) = C^+ f(t) g(\sigma) h(T)$ . Obviously, factorizability would offer an essential simplification of the description of creep under various conditions. While  $h(T)$  is usually identified with the Arrhenius or WLF equation, several empirical functions have been proposed for  $f(t)$  and  $g(\sigma)$  (they are reviewed in references 34 and 37). Clearly, the parameters of an applied empirical equation are determined *a posteriori* by fitting experimental data.

Short-term isothermal creep of polymers in the region of a linear stress-strain relationship was successfully analyzed (37, 38) using the Kohlrausch-Williams-Watts (KWW) function as an empirical fit to experimental data:

$$\epsilon(t) = \epsilon_{to} \exp(t/\tau_r)^n, \quad (2)$$

where  $\epsilon_{to}$  is a limiting deformation at short times,  $\tau_r$  is the mean retardation time and  $0 \leq n \leq 1$  is the creep curve shape parameter reflecting the distribution of retardation times. Isothermal nonlinear creep of polymers was in many papers (16, 39–44) plausibly described by a simple power law

$$\epsilon(t, \sigma) = C^* \sigma^m t^n, \quad (3)$$

where  $C^*$  is a constant,  $1 \leq m$  and  $n$  are empirical parameters. Also, nonlinear creep behavior of PP was found (45) to obey a similar equation:

$$\epsilon(t, \sigma) = A(\sigma) (t/\tau_r)^n, \quad (4)$$

where  $A(\sigma)$  is a nonlinear function of the stress and  $0 \leq n \leq 1$  is assumed to be independent of the applied stress.

Apparently more rigorous equations separating the elastic  $\epsilon_o(\sigma)$  (which can be obtained by extrapolation of  $\epsilon(t, \sigma, T)$  for  $t = 0$ ) and viscoelastic  $\epsilon_v(t, \sigma) = \epsilon(t, \sigma) - \epsilon_o(\sigma)$  components of strain were applied in a number of papers (34, 35, 46–50). It is worth noting that analogous functions were proposed for both  $\epsilon(t, \sigma)$  and  $\epsilon_v(t, \sigma)$ :

$$\epsilon_v(t, \sigma) = \epsilon^*(\sigma) t^n, \quad (5)$$

$$\epsilon_v(t, \sigma) = C' \sigma^m t^n, \quad (6)$$

$$\epsilon_v(t, \sigma) = C'' \sin h(\sigma/\sigma_{re}) t^n, \quad (7)$$

where  $\epsilon^*(\sigma)$  is a constant for a given stress,  $\sigma_{re}$  is a reference stress and  $C'$  or  $C''$  are empirical constants.

As can be seen, parameter  $n$  in Eqs 3–7 can be formally related to the creep rate:

$$d\epsilon(t)/dt \approx n t^{(n-1)}. \quad (8)$$

### Creep of Heterogeneous Binary Blends in Terms of the Equivalent Box Model

The proposed predictive scheme is based on a combination of a two-parameter equivalent box model (EBM) (Fig. 1) and the data on the phase continuity of components obtained from modified equations of the percolation theory. (It should be noted that “phase continuity” or “phase connectivity” may have different meanings in other papers.) Standard polymer blends are isotropic materials with three-dimensional continuity of one or more components so that series or parallel models as well as models for orthotropic or quasi-isotropic materials are not applicable. Thus more complex models appropriately combining both parallel and series couplings of constituents should be introduced (1–15). However, the EBM’s are not self-consistent models, so it is necessary to evaluate their parameters (volume fractions  $v_{ij}$ ) in an independent way. In brief, if we intend to use the EBM for the prediction of physical properties of blends, we must 1) derive the equations for the properties under consideration and 2) calculate the volume fractions  $v_{ij}$  (Fig. 1). The EBM assumes that either component can be modeled as consisting of a fraction continuous in the direction of the acting force ( $v_{1p}$  or  $v_{2p}$ ) and a fraction discontinuous in that direction ( $v_{1s}$  or  $v_{2s}$ ). Fractions  $v_{1p}$  and  $v_{2p}$  form the parallel branch (being coupled in parallel to the acting stress), fractions  $v_{1s}$  and  $v_{2s}$  form the series branch (being coupled in series); these two branches, each consisting of two blocks, are coupled in parallel.

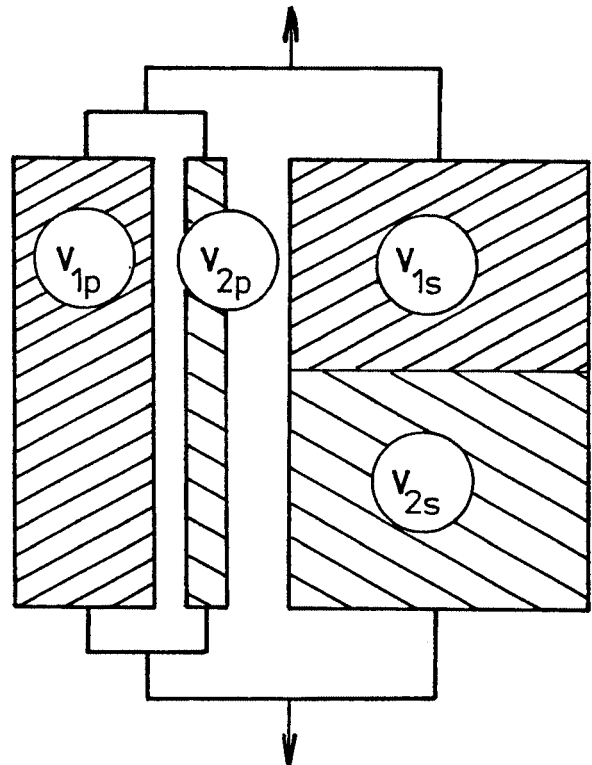


Fig. 1. Equivalent box model for a binary blend 60/40.

The EBM in Fig. 1 is a two-parameter model as of four fractions  $v_{ij}$  only two are independent. The blocks in the EBM are presumed to have mechanical properties of neat components; the model is likely to fail if the blending process produces a significant change in the structure (e.g., in crystallinity) and, consequently, in considered properties of a constituent.

Compliance of the parallel branch  $D_p(t)$  or of the series branch  $D_s(t)$  of the EBM (Fig. 1) is related to the compliance of components in the following manner (cf. ref. 1, 39, 15):

$$(v_{1p} + v_{2p})/D_p(t) = v_{1p}/D_1(t) + v_{2p}/D_2(t); \quad (9a)$$

$$(v_{1s} + v_{2s}) D_s(t) = v_{1s} D_1(t) + v_{2s} D_2(t). \quad (9b)$$

The resulting compliance of heterogeneous two-component blends is then given as the sum of the contributions of the parallel and series branches; i.e.,  $D_b(t) = [(v_{1p} + v_{2p})/D_p(t) + (v_{1s} + v_{2s})/D_s(t)]^{-1}$ :

$$D_b(t) = \{v_{1p}/D_1(t) + v_{2p}/D_2(t) + (v_{1s} + v_{2s})^2/[D_1(t) v_{1s} + D_2(t) v_{2s}]\}^{-1}. \quad (10)$$

To describe the compliance of blends with one continuous component and one discontinuous component, we can modify equations derived for modulus of particulate systems. If the minority polymer 2 of the volume fraction  $v_2$  having a lower compliance  $D_2(t) < D_1(t)$  is dispersed in polymer 1, the compliance  $D_{b1}(t)$  of the blend can be expressed by using the Kerner-Nielsen equation (16):

$$D_{b1}(t) = D_1(t) (1 - B_1\psi_1 v_2)/(1 + A_1 B_1 v_2). \quad (11a)$$

The quantities are defined (16) as follows:  $A_1 = (7 - 5 v_1)/(8 - 10 v_1)$  where  $v_1$  is the Poisson ratio of the matrix;  $B_1(t) = [D_1(t)/D_2(t) - 1]/[D_1(t)/D_2(t) + A_1]$ ;  $\psi_1 = 1 + [(1 - v_{2max})/v_{2max}^2] v_2$ , where  $v_{2max}$  is the maximum packing fraction of the particles of component 2. If the component 1 is dispersed, e.g., as in *rubber-toughened plastics*, then inverted relations hold for  $D_2(t) < D_1(t)$ :

$$D_{b2}(t) = D_2(t) (1 + A_2 B_2 v_1)/(1 - B_2 \psi_2 v_1). \quad (11b)$$

where  $A_2 = (8 - 10 v_2)/(7 - 5 v_2)$ ;  $B_2(t) = [D_1(t)/D_2(t) - 1]/[D_1(t)/D_2(t) + A_2]$ ;  $\psi_2$  is analogous to  $\psi_1$ .

### Calculation of the Volume Fractions of the EBM

The second step of the outlined scheme is the evaluation of  $v_{ij}$  defined in Fig. 1. Percolation theory (33, 51) provides a universal formula for the elastic modulus (or compliance) of binary systems where the contribution of the second component is negligible (in the following text we will use the original notation for modulus):

$$E_{1b} = E_a (v - v_{1cr})^q \quad (12)$$

where  $E_a$  is a constant,  $v_{1cr}$  is the critical volume fraction (the percolation threshold) and  $q$  is the critical universal exponent.  $E_{1b}$  stands for the modulus of a "single-component" blend in which the component 1

assumes the same phase structure as in the blend with component 2. Equation 12 was shown (3, 30) to plausibly fit the modulus of model blends with  $E_1 \gg E_2$  in the range  $v_{1cr} < v_1 \leq 1$ . Utilizing this experimental finding we can modify Eq 12 to the following form:

$$E_{1b} = E_1 [(v_1 - v_{1cr})/(1 - v_{1cr})]^{q_1}; \quad (13)$$

where  $E_1 = E_a (1 - v_{1cr})^{q_1}$  is the modulus of the neat component 1. If  $E_1 \gg E_2$ , the contribution  $E_2 v_{2p}$  of that part of component 2 which is coupled in parallel and the contribution of the whole series branch (Fig. 1) to the modulus of the EBM are negligible in comparison to the contribution  $E_1 v_{1p}$  of component 1. Consequently,  $E_1 v_{1p}$  (or  $E_2 v_{2p}$  for  $E_2 \gg E_1$ ) can be set equal to the apparent modulus  $E_{1b}$  (or  $E_{2b}$ ), i.e.,  $E_{1b} = E_1 v_{1p}$ ;  $E_{2b} = E_2 v_{2p}$ . Comparing these relations with Eq 13, we obtain expressions for  $v_{1p}$  and  $v_{2p}$ :

$$v_{1p} = [(v_1 - v_{1cr})/(1 - v_{1cr})]^{q_1}; \quad (14a)$$

$$v_{2p} = [(v_2 - v_{2cr})/(1 - v_{2cr})]^{q_2}; \quad (14b)$$

The remaining volume fractions  $v_{1s}$  and  $v_{2s}$  can be evaluated by using some of the following relations:

$$v_1 = v_{1p} + v_{1s}; \quad v_2 = v_{2p} + v_{2s}; \quad v_p = v_{1p} + v_{2p}; \\ v_s = v_{1s} + v_{2s}; \quad v_1 + v_2 = v_p + v_s = 1. \quad (15)$$

Most ascertained values of  $q$  are located in an interval of 1.6–2.0 so that  $q = 1.8$  can be used as an average value (1, 3, 51, 52). For three-dimensional cubic lattice, the percolation threshold  $v_{cr} = 0.156$  was calculated (33, 51, 52). In general, the patterns predicted by using "universal" values  $v_{1cr} = v_{2cr} = 0.156$  and  $q_1 = q_2 = 1.8$  should be viewed as a first approximation that may not be in a good accord with experimental data because  $v_{1cr}$  and  $v_{2cr}$  of polymer blends frequently differ from 0.156 and from each other. Vice versa, as soon as some experimental data on physical properties of blends are available, more precise values of  $v_{1cr}$  and  $v_{2cr}$  can be obtained by a fitting procedure. In this way, the EBM may become a source of quantitative information on the phase duality in polymer blends.

## RESULTS AND DISCUSSION

In order to ascertain the stress-strain linearity limit for parent polymers and their blends, short-term creep (lasting 100 min) was performed for a series of stresses increased step-by-step in the interval 2.7–16.2 MPa for RTPP (subscript 1) and 2.7–27 MPa for SAN (subscript 2). In the case of RTPP (not all measured curves can be given in Fig. 2 for clarity reasons), we can distinguish three types of creep behavior:

1) the  $\log D_1(t)$  vs.  $\log t$  plot is independent of stress at  $\sigma < \text{about } 5 \text{ MPa}$  and can be approximated by a straight line, i.e.,  $n_1$  of Eq 3 is a constant independent of stress. As can be seen, the corresponding dependencies  $\log D_{1v}(t)$  vs.  $\log t$  markedly deviate from a straight line.

2) in the interval  $5 \text{ MPa} < \sigma < \sim 10 \text{ MPa}$ , the  $\log D_1(t)$  vs.  $\log t$  plot can be still approximated by a straight

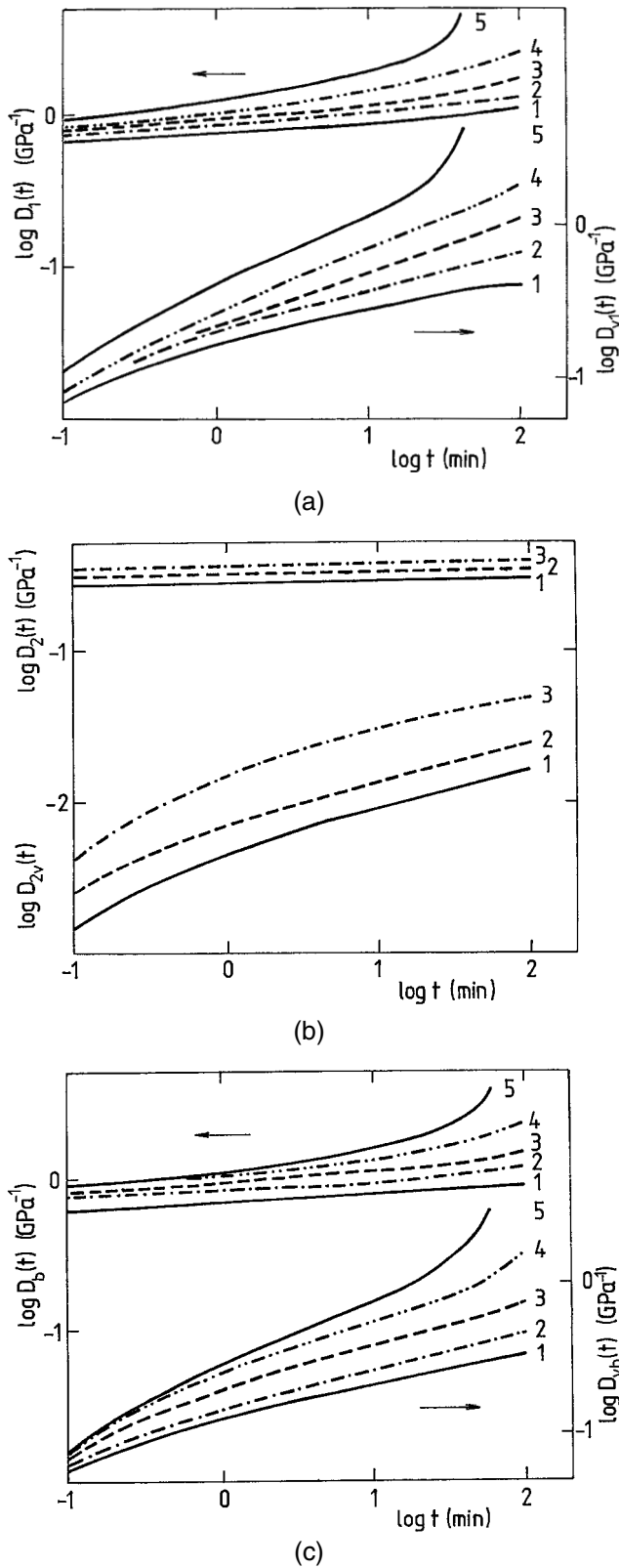


Fig. 2. Short-term creep: effect of tensile stress (in MPa) on the compliance  $D(t)$  (upper curves) and viscoelastic component of compliance  $D_v(t)$  (lower curves); a) RTTP: (1) 2.7; (2) 8.1; (3) 10.8; (4) 13.5; (5) 16.2; b) SAN: (1) 5.4; (2) 16.2; (3) 27; c) RTTP/SAN = 85/15 blend: (1) 2.7; (2) 8.1; (3) 13.5; (4) 16.2; (5) 18.9.

line, but the rising stress increases not only  $C_1^*(\sigma) = D_1(t=1)$  (as expected), but also the slope of the straight line, i.e.,  $n_1 = n_1(\sigma)$ , which is virtually independent of time. Similarly to the previous case, the dependencies  $\log D_{1,v}(t)$  vs.  $\log t$  are not linear.

3) at  $\sigma > 10$  MPa,  $C_1^*(\sigma)$  continues rising with acting stress; moreover, an increase in the derivative  $d[\log D_1(t)]/d[\log(t)]$  can be observed with the elapsed time of creeping, i.e., parameter  $n_1 = n_1(\sigma, t)$  rises with (i) the stress and (ii) the elapsed time of creep experiments. On the other hand, none of the corresponding dependencies  $\log D_{1,v}(t)$  vs.  $\log t$  can be approximated by a straight line. At the highest applied stress (16.2 MPa), the creep of RTTP profoundly accelerates after about 30 min because the yield strength has obviously been exceeded (however, the deformation remains homogeneous, i.e., without neck formation). Complex creep behavior of RTTP is likely to be associated with complex phase structure because RTTP consists of three phases and can hardly be expected to perform as a rheologically simple material. A rather complicated creep behavior was observed earlier even for neat PP (53).

SAN shows (Fig. 2b) a creep behavior contrasting to that of RTTP:  $D_2(t)$  is practically independent of time (in the interval 0.1–100 min) and of stress (up to 21.6 MPa); at  $\sigma = 27$  MPa, the observed compliance is somewhat higher. Consequently,  $D_{2,v}(t)$  is very low, corresponding to only a few percents of  $D_2(t)$ . Obviously, the compliance of SAN is virtually independent of time and stress in the studied intervals because the polymer is in the glassy state at the temperature of creep measurements. The propensity to creep of parent polymers is very different as  $n_1 = 0.105$  for RTTP while  $n_2 = 0.005$  for SAN (Table 1); thus, SAN can be viewed as a low-creep polymer (54).

As SAN prevalingly displays a time-independent elastic behavior, we can expect that viscoelastic effects characterizing blends are associated with the RTTP component. For instance, stress affects the time dependencies of  $D_b(t)$  and  $D_{b,v}(t)$  of the blend RTTP/SAN = 85/15 (Fig. 2c) in a similar way to those of RTTP (Fig. 2a). The volume fraction of SAN  $v_2 = 0.13$  in this blend lies approximately in the middle of the studied composition interval ( $0 \leq v_2 \leq 0.27$ ) and corresponds to the critical volume fraction  $v_{2cr}$  of SAN in the studied series of blends as found in our preceding paper (15). Similarly to the neat RTTP, the 85/15 blend shows a linear dependence  $\log D_b(t)$  vs.  $\log t$  only at low stresses, i.e.,  $\sigma < 5$  MPa. The slope of the dependence slightly increases with applied stress for  $5 < \sigma < \sim 13$  MPa. At stresses  $\sigma \geq 13.5$  MPa, the parameter  $n_b(\sigma, t)$  rises with the time in the course of creep experiments. Quite analogous effects of stress on creep behavior were observed also for the other blends RTTP/SAN. Obviously, the factorizability of the effects of time and stress is rather questionable in the case of the studied blends.

In this paper, the simplest case, i.e., the creep behavior in the region of the linear stress-strain relationship,

**Table 1. Parameters of Eq 3 for the Creep Compliance of Rubber-Toughened Polypropylene, Poly(styrene-co-acrylonitrile) and Their Blends.**

RTPP/SAN weight %	$v_2$ vol. fract	Parameter $C_b$			Parameter $n_b$		
		tensile	flexural	calculated	tensile	flexural	calculated
100/0	0	0.88	0.78	—	0.105	0.103	—
95/5	0.043	0.80	0.68	0.84*	0.099	0.096	0.098*
90/10	0.087	0.80	0.75	0.80*	0.093	0.085	0.090*
85/15	0.131	0.82	0.75	0.76	0.085	0.073	0.092
80/20	0.176	0.76	0.58	0.71	0.075	0.073	0.084
75/25	0.222	0.67	0.58	0.67	0.072	0.062	0.075
70/30	0.268	0.65	0.59	0.63	0.065	0.064	0.067
0/100	1	0.29	0.8	—	0.005	0.007	—

\*Equation 11a was used instead of Eq 10 for the calculation of  $C_b$  and  $n_b$  (see the text).

will be discussed on the basis of long-term experiments performed at low stresses, i.e.,  $\sigma < 5$  MPa (Fig. 3). The stress acting in flexural creep can be calculated by using the relation (54):

$$\sigma = 3FL/2bh^2 \quad (16)$$

where  $F$  is the mid-span load,  $L$  is the span length,  $b$  is the width and  $h$  is the thickness of the specimen.  $D(t)$  and  $D_v(t)$  found in flexure are systematically somewhat lower than the values ascertained in tension, but the corresponding curves are parallel (Fig. 3). There are several factors affecting the compliance observed in flexural tests: 1) a stress gradient exists in the flexural specimens (53) where the maximum tensile stress given by Eq 16 acts only in the outer layer, while decreases to zero in the neutral axis and becomes compressive towards the loaded surface; 2) plastics do not perfectly obey the assumptions of the classical theory of linear elasticity (55); 3) the “skin” layer containing less minority component than the “core” plays a more important role than in tensile tests; however, a quantitative evaluation of the difference would be very difficult.

For the following analysis of the creep behavior of blends we will use  $D_b(t)$  because  $D_{bv}(t)$  can hardly be approximated by a simple equations (for calculating  $D_{bv}(t)$ , it would be inevitable to employ numerical data of  $D_{1v}(t)$  and  $D_{2v}(t)$  of components). Besides,  $D_b(t)$  is a much more practical function than  $D_{bv}(t)$ . To fit and/or to predict the straight lines  $D_b(t)$  vs.  $\log(t)$  we will use Eq 3 (with  $m = 1$ ), which ranks among the simplest empirical equations because it contains only two adjustable parameters. Linear dependencies  $\log D_b(t) - \log(t)$  (Fig. 3) can be approximated by Eq 3 with a plausible accuracy for parent polymers and their blends in both types of creep tests. In this paper we intend (i) to compare experimental and calculated data of  $C_b$  and  $n_b$  and (ii) to predict a complete creep curve of a blend by using the parameters  $C_1$ ,  $n_1$ ,  $C_2$  and  $n_2$  found for parent polymers (Table 1) as the only experimental input data. We will assume that, in addition to  $\log D_1(t) = \log C_1 + n_1 \log t$  and  $\log D_2(t) = \log C_2 + n_2 \log t$  valid for the parent polymers, also  $\log D_b(t) = \log C_b + n_b \log t$  holds for a blend. Introducing these relations into Eq 10 and assuming  $t = 1$  we obtain the relation between  $C_1$ ,  $C_2$  and  $C_b$ :

$$C_b = [(v_{1p}/C_1) + (v_{2p}/C_2) + (v_{1s} + v_{2s})^2/(v_{1s}C_1 + v_{2s}C_2)]^{-1} \quad (17)$$

The compliance of a blend is then given (for  $t \neq 1$ ) as

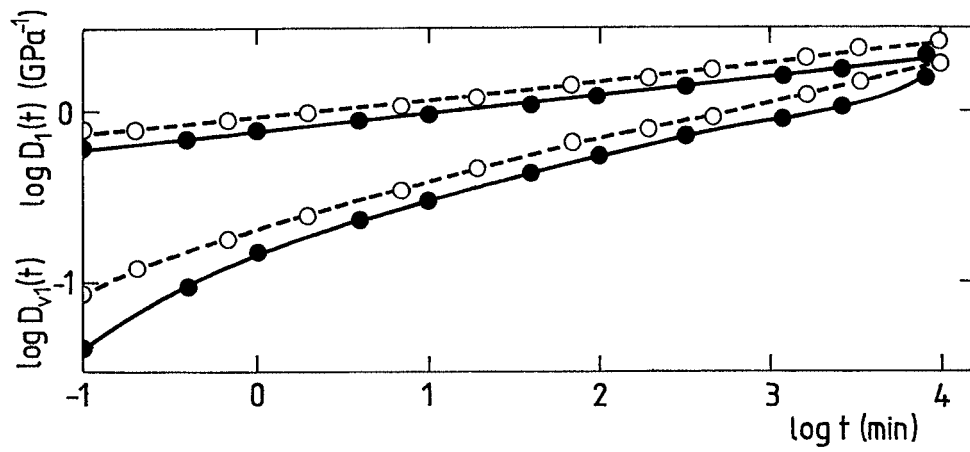
$$\begin{aligned} \log D_b(t) &= \log [(v_{1p}/C_1 t^{n_1}) + (v_{2p}/C_2 t^{n_2}) \\ &+ (v_{1s} + v_{2s})^2/(v_{1s}C_1 t^{n_1} + v_{2s}C_2 t^{n_2})]^{-1} \\ &= \log C_b + n_b \log t \end{aligned} \quad (18)$$

The relation between  $n_1$ ,  $n_2$  and  $n_b$  assumes the following form (for  $t \neq 1$ ):

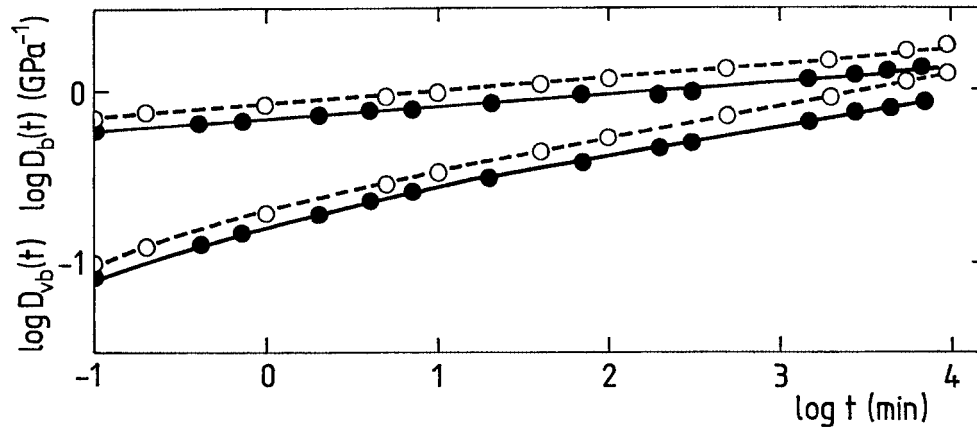
$$n_b = [\log D_b(t) - \log C_b]/\log t \quad (19)$$

Table 1 shows that experimental values of  $C_b$  from flexural creep are systematically somewhat lower than  $C_b$  from tensile experiments, which is a consequence of lower values of the compliance in flexure (Fig. 3). The values of  $C_b$  calculated from Eq 17 (for  $C_1 = 0.88$  and  $C_2 = 0.29$  found for components) are in an acceptable accord with experimental data. On the other hand, Eq 19 indicates that the parameter  $n_b$  predicted by the EBM is a function of the time of creeping though  $n_1$  and  $n_2$  are assumed to be time-independent constants. Figure 4 shows (on a very extended scale) that the calculated  $n_b$  only slightly decreases with time. (The values of  $n_b$  given in Table 1 were calculated from Eq 19 for  $\log t = 3$ .) For  $v_2 < v_{2cr} = 0.13$ , Eq 11a was used instead of Eq 10 in calculating  $C_b$  and  $n_b$ ; probably for this reason,  $n_b$  for  $v_2 = 0.087$  is somewhat lower than  $n_b$  for  $v_2 = 0.131$  (Table 1). As can be seen,  $n_b$  gets smaller with rising fraction of SAN and fairly well corresponds to experimental values characterizing tensile creep. Experimental  $n_b$ 's from flexural creep are somewhat lower than those from tensile measurements but the differences are not significant. The values of  $n_b$  do not seem to be distinctly reduced (Table 1) at volume fractions  $v_2 > 0.13 = v_{2cr}$ , where SAN assumes a partial phase continuity. As  $n_b \ll 1$ , the creep rate of the studied blends diminishes in the course of creep.

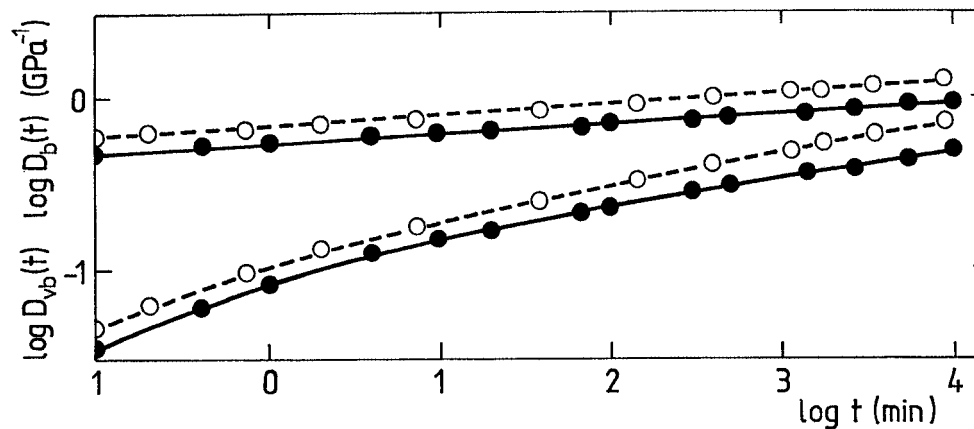
In Fig. 4, the  $\log D(t)_b$  vs.  $\log t$  dependence for the RTPP/SAN = 80/20 blend is predicted throughout the time interval 0.1–10,000 min according to Eq 18 by using the experimentally found parameters  $C_1$ ,  $n_1$ ,  $C_2$  and  $n_2$  characterizing the constituents. The calculated curve is in a good accord with experimental data over



(a)



(b)



(c)

Fig. 3. Long-term creep: compliance  $D(t)$  (upper curves) and viscoelastic component of compliance  $D_v(t)$  (lower curves) in tension (full lines) and flexure (dashed lines); a) RTPP: tensile stress: 6.75 MPa; stress in flexure: 5.15 MPa in all tests; b) RTPP/SAN = 85/15 blend: tensile stress: 9.45 MPa; c) RTPP/SAN = 70/30 blend: tensile stress: 12.15 MPa.

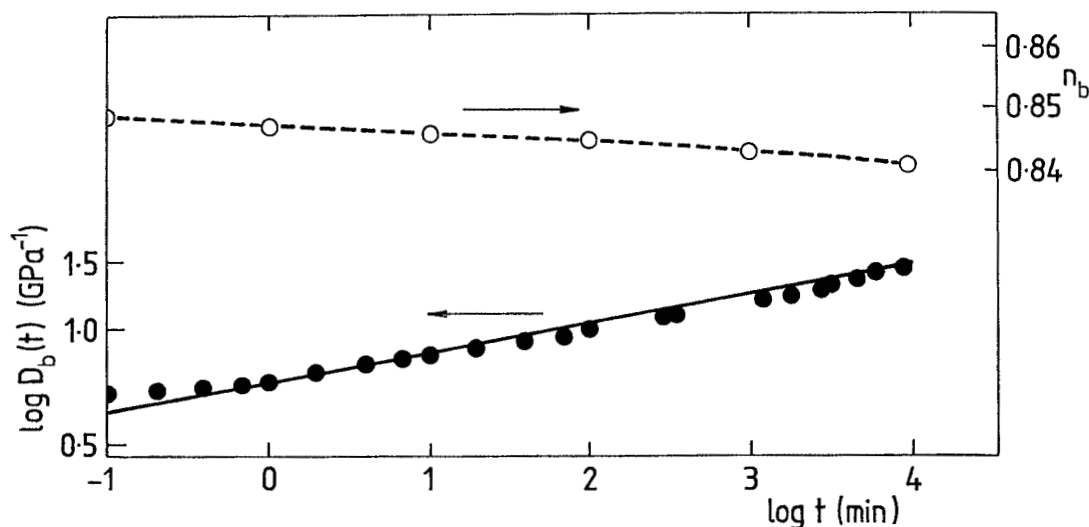


Fig. 4. Long-term creep of the RTPP/SAN = 80/20 blend: compliance  $D_b(t)$  (full line) calculated from Eq 18 and parameter  $n_b$  (empty circles, dashed line) calculated from Eq 19 as functions of time. Input parameters:  $C_1 = 0.88$ ,  $C_2 = 0.29$ ,  $n_1 = 0.105$ ,  $n_2 = 0.005$  (Table 1),  $v_{1cr} = 0.16$ ,  $v_{2cr} = 0.13$ ,  $q_1 = q_2 = 1.2$  (cf. ref. 15). Full circles—experimental data for tensile creep.

the whole time interval of creep measurements. Thus we can conclude that the EBM and the percolation approach to the phase continuity form a good basis for the predictive format for the creep of heterogeneous polymer blends.

### CONCLUSIONS

A previously proposed predictive format for the elastic, storage and loss moduli has been extended for the time-dependent compliance  $D_b(t)$  of polymer blends. The format employs a two-parameter equivalent box model (EBM) and the data on the phase continuity of components in blends obtained by using modified equations of the percolation theory. The only input data are the compliances  $D_1(t)$  and  $D_2(t)$  and the critical volume fractions  $v_{1cr}$  and  $v_{2cr}$  (delimiting the interval of phase co-continuity in blends) of components. The time dependencies of  $D_1(t)$ ,  $D_2(t)$  and  $D_b(t)$  within the linear stress-strain region have been fitted by a simple empirical equation proposed earlier by other authors. Applicability of the outlined format has been verified for blends consisting of components with markedly different viscoelastic properties, namely rubber-toughened polypropylene and poly(styrene-co-acrylonitrile). The proposed format predicts fairly well the creep behavior of the mentioned blends over the studied interval 0.1–10,000 minutes. Thus the EBM and the percolation approach to the phase continuity in polymer blends constitute a unique predictive format suitable for the creep of heterogeneous polymer blends. The format is believed to allow the experimentalists to anticipate, at least semi-quantitatively, the creep behavior of intended blends.

### ACKNOWLEDGMENT

The first author is greatly indebted to the Grant Agency of the Czech Republic for financial support of this work (Grant No. 106/98/0700).

Travel expenses of collaborating parties were partly covered by the Ministry of Education of the Czech Republic and by the Ministry of Foreign Affairs of Italy under the 1st Joint Program on Scientific and Technological Cooperation.

### REFERENCES

1. J. Kolařík, *Polym. Networks Blends*, **5**, 87 (1995).
2. J. Kolařík, *Polymer*, **37**, 887 (1996).
3. J. Kolařík, *Polym. Eng. Sci.*, **36**, 2518 (1996).
4. J. Kolařík, F. Lednický, G. C. Locati, and L. Fambri, *Polym. Eng. Sci.*, **37**, 128 (1997).
5. J. Kolařík and G. Geuskens, *Polym. Networks Blends*, **7**, 13 (1997).
6. J. Kolařík, G. C. Locati, L. Fambri, and A. Penati, *Polym. Networks Blends*, **7**, 103 (1997).
7. J. Kolařík, *Polym. Compos.*, **18**, 433 (1997).
8. Z. Horák, J. Kolařík, M. Šípek, V. Hynek, and F. Večerka, *J. Appl. Polym. Sci.*, **69**, 2615 (1998).
9. J. Kolařík, *Eur. Polym. J.*, **34**, 585 (1998).
10. L. Matějka, O. Duch, and J. Kolařík, *Polymer*, **41**, 1449 (1999).
11. J. Kolařík, *J. Macromol. Sci.-Phys.*, **B39**, 53 (2000).
12. J. Kolařík, L. Fambri, A. Pegoretti, and A. Penati, *Polym. Eng. Sci.*, **40**, 127 (2000).
13. J. Kolařík, L. Fambri, A. Pegoretti, and A. Penati, *Polym. Adv. Technol.*, **11**, 1 (2000).
14. J. Kolařík and L. Fambri, *Macromol. Mater. Eng.*, **283**, 41 (2000).
15. J. Kolařík, A. Pegoretti, L. Fambri, and A. Penati, *J. Polym. Res.*, **7**, 1 (2000).
16. L. E. Nielsen and R. F. Landel, *Mechanical Properties of Polymers and Composites*, M. Dekker, New York (1994).



17. L. A. Utracki, *Polymer Alloys and Blends*, Hanser Publ., Munich (1990).
18. M. J. Folkes and P. S. Hope, *Polymer Blends and Alloys*, Chapman & Hall, Cambridge (1993).
19. L. H. Sperling, *Polymeric Multicomponent Materials*, Wiley, New York (1997).
20. D. R. Paul and C. B. Bucknall, eds., *Polymer Blends*, Wiley, New York (1999).
21. C. B. Bucknall, D. Clayton, and W. E. Keast, *J. Mater. Sci.*, **7**, 1443 (1972).
22. C. B. Bucknall and I. C. Drinkwater, *J. Mater. Sci.*, **8**, 1800 (1973).
23. C. B. Bucknall and C. J. Page, *J. Mater. Sci.*, **17**, 808 (1982).
24. H. Oysaed and I. E. Ruyter, *J. Biomed. Mater. Res.*, **23**, 719 (1989).
25. H. Gramespacher and J. Meissner, *J. Rheol.*, **39**, 151 (1995).
26. P. Mariani, R. Frassine, M. Rink, and A. Pavan, *Polym. Eng. Sci.*, **36**, 2750 (1996).
27. A. Lee and G. B. McKenna, *J. Polym. Sci. B: Polym. Phys.*, **35**, 1167 (1997).
28. L. A. Utracki, *J. Rheol.*, **35**, 1615 (1991).
29. J. Lyngaae-Jorgensen and L. A. Utracki, *Makromol. Chem., Macromol. Symp.*, **48/49**, 189 (1991).
30. J. Lyngaae-Jorgensen, A. Kuta, K. Sondergaard, and K. V. Poulsen, *Polym. Networks Blends*, **3**, 1 (1993).
31. G. Menges and H. J. Roskothen, *Polym. Eng. Sci.*, **15**, 544 (1975).
32. D. W. Scott, J. S. Lai, and A. H. Zureick, *J. Reinf. Plast. Compos.*, **14**, 588 (1995).
33. P. G. De Gennes, *J. Phys. Lett. (Paris)*, **37**, L1 (1976).
34. M. Schlimmer, *Rheol. Acta*, **18**, 62 (1979).
35. F. Y. C. Boey, T. H. Lee, and K. A. Khor, *Polym. Testing*, **14**, 425 (1995).
36. J. X. Li and W. L. Cheung, *J. Appl. Polym. Sci.*, **56**, 881 (1995).
37. P. E. Tomlins, *Polymer*, **37**, 3907 (1996).
38. L. C. E. Struik, *Polymer*, **30**, 799 (1989).
39. D. W. Cruickshanks-Boyd and N. Roswati, *J. Biomed. Mater. Res.*, **15**, 769 (1981).
40. N. Brown, J. Donofrio, and X. Lu, *Polymer*, **28**, 1326 (1987).
41. N. Verdonshot and R. Huiskens, *J. Biomed. Mater. Res.*, **29**, 575 (1995).
42. N. Mukherjee, M. Dharia, and R. Rajan, *J. Reinf. Plast. Compos.*, **17**, 51 (1999).
43. J. Horský, J. Kolařík, and L. Fambri, *Angew. Makromol. Chem.*, **264**, 39 (1999).
44. J. Horský, J. Kolařík, and L. Fambri, *Angew. Makromol. Chem.*, **271**, 75 (1999).
45. R. W. Garbella, J. Wachter, and J. H. Wendorff, *Progr. Coll. Polym. Sci.*, **71**, 164 (1985).
46. W. N. Findley, *Polym. Eng. Sci.*, **27**, 582 (1987).
47. D. A. Dillard, M. R. Straight, and H. F. Brinson, *Polym. Eng. Sci.*, **27**, 116 (1987).
48. C. Migliaresi, L. Fambri, and J. Kolařík, *Biomaterials*, **15**, 875 (1994).
49. W. J. Liou and C. I. Tseng, *Polym. Compos.*, **18**, 492 (1997).
50. C. J. Carriere, D. Bank, and M. Malanga, *J. Appl. Polym. Sci.*, **67**, 1177 (1998).
51. W. Y. Hsu and S. Wu, *Polym. Eng. Sci.*, **33**, 293 (1993).
52. J. Sax and J. M. Ottino, *Polym. Eng. Sci.*, **23**, 165 (1983).
53. R. J. Crawford, *Plastics Engineering*, Butterworth-Heinemann, Oxford (1998).
54. B. Xu, J. Simonsen, and W. E. Rochefort, *J. Appl. Polym. Sci.*, **76**, 1100 (2000).
55. I. D. McCay, *J. Appl. Polym. Sci.*, **42**, 281 (1991).